Diurnal Parallax Determinations of Asteroid Distances Using Only Backyard Observations from a Single Station

Eduardo Manuel Alvarez
Observatorio Los Algarrobos, Salto, Uruguay
Costanera Sur 559, Salto 50.000, URUGUAY
olasu@adinet.com.uy

Robert K. Buchheim
Altimira Observatory
Coto de Caza, CA 92679, USA
Bob@RKBuchheim.org

Abstract

A method of using diurnal parallax for determining the distance to asteroids has been developed, which provides excellent accuracy using an amateur-level telescope and CCD, and a surprisingly simple set of observations. Data from two consecutive nights is sufficient, obtained at the beginning of each night, and at each culmination. Just those few data points proved to be enough to allow computing accurately (better than 5%) the distance to the asteroid. Results for several asteroids will be shown.

1. Introduction

The direct comparison of two observations of a relatively near object obtained at exactly the same time from two different stations, where it shows some angular displacement (parallax) with respect to the distant background stars, is a well-known exercise in positional astronomy (astrometry). In fact, as early as 1672 Cassini was able to demonstrate its full validity by achieving quite good results for Mars' parallax – although the extensive travel, and years of preparation and data reduction that this required are testimony to just how difficult a proposition it was!

The advent of photography made this parallax issue far more practical, and the use of CCD cameras made it far more accurate.

Twenty years ago Ratcliff and colleagues reported that they had successfully made parallax observations of two asteroids by this method (Ratcliff et al., 1993). Those pioneering measurements were accomplished after a careful and long preparation, involving the joint and synchronized work of two research observatories. Several years later the measurement of asteroid parallax by means of small telescopes was addressed in detail for Near Earth Objects (NEO) (Smallwood *et al.*, 2004), who exclusively referred to simultaneous measurements obtained from two stations.

In contrast, the method of diurnal parallax requires only a single observing site, and uses a baseline that is provided by the rotation of the Earth. This is also a historically significant and a simpler method to use (compared to the two-station parallax). It seems to have been first successfully applied to the solar system by Flamsteed in 1672, to measure the parallax of Mars (Forbes, 1976) and later by Lindsay and Gill, when they measured the parallax of Juno in 1874 (Lindsay and Gill, 1877).

The possibility that amateurs could use the diurnal parallax effect for determining Solar System distances from CCD images obtained from just one single observing point has been recently discussed in practical terms by Vanderbei and Belikov (2007) and Buchheim (2011). However, both approaches present drawbacks – the first one requiring precise orbital data which is not obtained by the observer himself; the latter only dealing with a particular case.

The question that we posed was whether a general self-contained practical method for determining asteroid distances via parallax by means of CCD images obtained from just one vantage point could be possible. By "self-contained" we emphasize the condition that all required data for the distance computation must be obtained from direct observations – not from third party data. (If one requires extra technical information for determining an object's distance, the used method seems to us to be a bit handicapped.) The idea was to develop a method that could accurately determine a Solar System object's distance from data gathered by just one observer. The good news is that we confidently think we have succeeded.

2. The Diurnal Parallax Effect

Parallax is a widely-understood and easily demonstrated phenomenon, as well as its derived practical benefit – to allow determining the distance to an object without directly measuring it. In astronomy, this fits like a glove. It has been used to determine the size of the Earth (Eratosthenes), the scale of the Solar System (during Venus' transits) and the distance to near-by stars (Hipparcos satellite).

In theory, once the parallactic shift of the apparent position of a distant object as observed from the ends of a baseline of known length is measured, then its distance can be readily determined. In practice, taking into account that in most astronomical applications the parallax angle is very small, the only way to improve the accuracy of the distance determination is by means of enlarging the baseline.

As already mentioned, parallactic measures simultaneously performed from two conveniently far away observatories have successfully yielded asteroid distances. The big question here is: can one single observer determine accurate asteroid distances by taking advantage of his relative displacement to the target due to Earth's rotation?

Placed on the Earth's surface, any observer is actually moving along a perfectly circular track, several thousand kilometers in radius, making one complete circle in almost 24 hours (sidereal period). At any given time, the observer sees the asteroid from a slightly different perspective compared to a fictitious observer placed at the center of the Earth. Those are the vantage points that play this particular parallax game. This variable parallax effect has nothing to do with the fact that the asteroid is also moving with respect to the Earth – it only refers to the different (and constantly changing) spatial position of the observer relative to the center of the Earth due to the Earth's rotation.

Assuming the asteroid's distance is fixed with respect to the Earth's center – except for NEO asteroids, a general pertinent assumption for time periods as short as half day to a couple of days – the time variability of the parallax angle due to observer location on the rotating Earth can be exclusively attributed to his changing position relative to a fixed direction in the equatorial plane. In other words, the parallax angle relative to the plane that contains the axis of rotation never changes.

This is the basis of the diurnal parallax definition – also called the east-west parallax. As shown in Figure 1, the diurnal parallax effect is the variable parallax due to the observer's daily rotation with respect to the Earth's center. It's clear that at the moment of the target's culmination (when the target happens to be on the observer's Meridian) the diurnal parallax angle becomes null, while achieving its maximum value 6 hours either before or after transit.

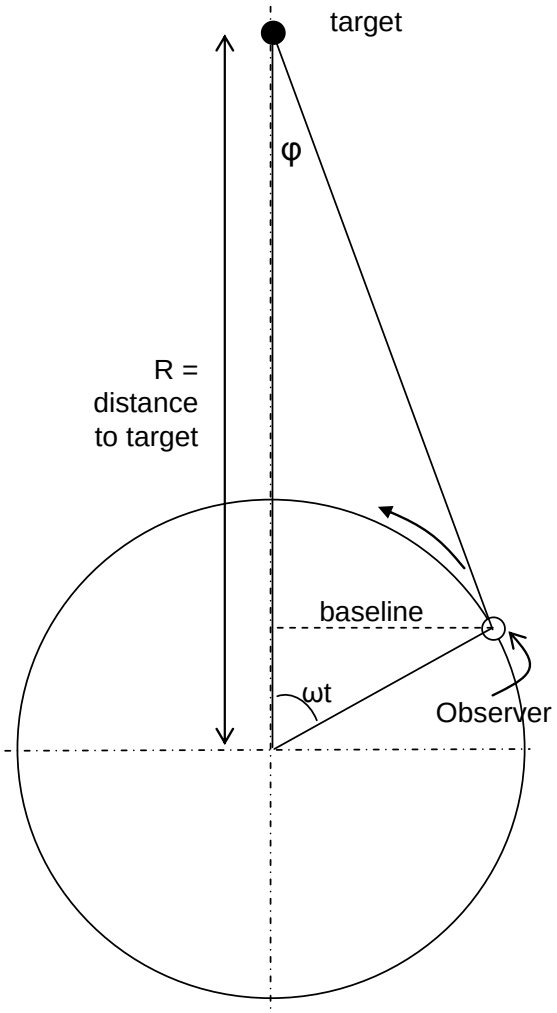

Figure 1 : Geometry of the diurnal parallax effect. As the Earth rotates, any observer on its surface sees the target's parallactic angle φ constantly varying, from a maximum value occurring whenever his Meridian is at right angle to the plane containing the Earth's rotation axis and the target (some 6 hours prior or after transit time) to a null value whenever the target is placed on his Meridian (target culmination).

The diurnal parallax becomes the angle that at any given moment has the target on its vertex, the observer on one side and the center of the Earth on the other side, projected to the equatorial plane. Therefore, by definition, at any given time *t* the diurnal parallax angle φ becomes

$$\varphi(t) = [RA_{topo}(t) - \alpha_{geo}(t)]\cos\delta(t) \qquad (1)$$

where RA_{topo} is the object's topocentric (measured from the observer location) right ascension, α_{geo} is the

object's geocentric (measured from the center of the Earth) right ascension, and δ is the object's declination (assumed to be practically the same as measured either from the observer's place or from the center of the Earth).

Once this angle is determined, and knowing the length of the corresponding projected observational baseline B, the distance to the asteroid R can be readily obtained by making use of the small-angle approximation:

$$R = \frac{B(t)}{\varphi(t)} \qquad (2)$$

where B and R are expressed in the same units and the angle φ is in radians. From Figure 1 the projected baseline is

$$B(t) = R_E \cos\lambda \cos(\omega t) \qquad (3)$$

where R_E is the radius of the Earth, λ is the latitude of the observer, and ω is the angular sidereal rotation rate of the Earth. Therefore, all that matters now is how to accurately determine the elusive diurnal parallax angle φ.

3. The Model

The geometry of our model is shown in Figure 2. The non-rotating coordinate frame is attached to the center of the Earth (geocentric frame). It is oriented so that the +Z-axis points toward celestial north, and the +X-axis points toward the position where the asteroid is at time $t = 0$. Because of the symmetry of the diurnal parallax effect we strategically select the beginning of the time parameter to coincide with the moment of the asteroid culmination. Hence,

$$t = T - T_0 \qquad (4)$$

where T is the "clock" time (this might be civil time or UT, depending on the preference of the observer) and T_0 is the exact time of the asteroid culmination (in the same timing reference).

At any time *t*, the geocentric position of the asteroid (which does move on the sky) is given by the vector ***R**(t)*:

$$\vec{R}(t) = \begin{bmatrix} x_R(t) \\ y_R(t) \\ z_R(t) \end{bmatrix} = \begin{bmatrix} R\cos\delta\cos\Delta\alpha \\ R\cos\delta\sin\Delta\alpha \\ R\sin\delta \end{bmatrix} \qquad (5)$$

where R is the geocentric distance of the asteroid, δ is the geocentric declination of the asteroid, and Δα is the angular difference in the geocentric right ascension of the asteroid measured from $t = 0$, thus becoming

$$\Delta\alpha(t) = \alpha_{geo}(t) - \alpha_0 \qquad (6)$$

where $\alpha_{geo}(t)$ is the geocentric right ascension of the asteroid at time *t*, and α_0 is the geocentric right ascension at the moment of the asteroid culmination. R, δ, and Δα are functions of time.

Considering that the observer sees the asteroid not from the Earth's center but from a different vantage point (as shown in Figure 2), necessarily the asteroid coordinates that he measures at any given time are (slightly) different from corresponding geocentric coordinates.

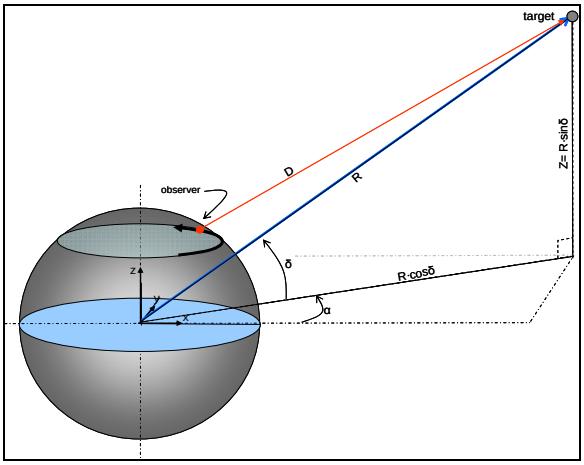

Figure 2: The spatially fixed geocentric frame. It's centered at the Earth center, the Z-axis coinciding with the Earth rotational axis and the X-axis pointing towards the direction that makes the plane XZ to also contain the target at the moment of its culmination.

At any time *t*, the geocentric position of the observer as he is carried around by the Earth's rotation is given by the vector ***r**(t)* (not shown in Figure 2). Assuming a spherical Earth, the vector ***r**(t)* is:

$$\vec{r}(t) = \begin{bmatrix} x_r(t) \\ y_r(t) \\ z_r \end{bmatrix} = \begin{bmatrix} R_E\cos\lambda\cos(\omega t) \\ R_E\cos\lambda\sin(\omega t) \\ R_E\sin\lambda \end{bmatrix} \qquad (7)$$

where R_E is the radius of the Earth, λ is the latitude of the observer, and ω is the angular sidereal rotation rate of the Earth.

The vector ***D**(t)* from the observer to the asteroid thus becomes:

$$\vec{D}(t) = \vec{R}(t) - \vec{r}(t) \tag{8}$$

so that

$$\vec{D}(t) = \begin{bmatrix} x_D(t) \\ y_D(t) \\ z_D(t) \end{bmatrix} = \begin{bmatrix} R\cos\delta\cos\alpha - R_E\cos\lambda\cos(\omega t) \\ R\cos\delta\sin\alpha - R_E\cos\lambda\sin(\omega t) \\ R\sin\delta - R_E\sin\lambda \end{bmatrix} \tag{9}$$

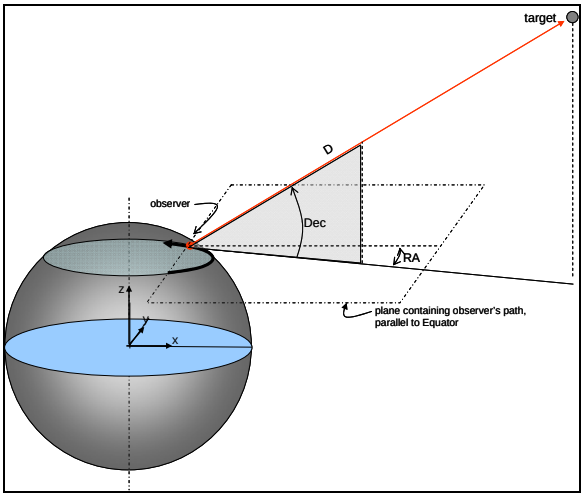

Figure 3: The moving topocentric frame. It's centered at the observer's location on the Earth's surface, but at any time its three axes are parallel to corresponding axes of the geocentric frame. Hence, the XY plane is always parallel to the Equatorial plane, and the XZ plane happens to coincide with the Meridian at the moment of the target's culmination.

Figure 3 shows a non-rotating coordinate frame centered on the observer's location on the surface of the Earth (topocentric frame). It is oriented so that both the +Z-axis and the +X-axis are parallel to corresponding axes in the geocentric frame. Hence, at time $t = 0$ the +X-axis also points toward the position where the asteroid is, which happens to be placed at the Meridian.

At any time t, the topocentric position of the asteroid is given by the vector $D(t)$:

$$\vec{D}(t) = \begin{bmatrix} x_D(t) \\ y_D(t) \\ z_D(t) \end{bmatrix} = \begin{bmatrix} D\cos(Dec)\cos(\Delta RA) \\ D\cos(Dec)\sin(\Delta RA) \\ D\sin(Dec) \end{bmatrix} \tag{10}$$

where D is the topocentric distance to the asteroid, Dec is the topocentric declination of the asteroid, and ΔRA is the angular difference in the topocentric right ascension of the asteroid measured from $t = 0$, thus becoming

$$\Delta RA(t) = RA_{topo}(t) - RA_0 \tag{11}$$

where $RA_{topo}(t)$ is the topocentric right ascension of the asteroid at time t, and RA_0 is the topocentric right ascension at the moment of the asteroid culmination. D, Dec, and ΔRA are functions of time.

From (10), dividing the y_D by the x_D coordinates of the vector $\boldsymbol{D}(t)$ and substituting the corresponding values from (6) it becomes

$$\frac{y_D}{x_D} = \tan(\Delta RA) = \frac{X\cos\delta\sin\Delta\alpha - \sin(\omega t)}{X\cos\delta\cos\Delta\alpha - \cos(\omega t)} \tag{12}$$

where

$$X = \frac{R}{R_E\cos\lambda} \tag{13}$$

Besides the goal distance R, Equation 12 still includes other unknown time-dependent parameters (δ and Δα) basically related to the actual asteroid motion on the sky. In order to simplify the asteroid distance computation, now we are going to make several important assumptions.

First of all, we assume that the asteroid's geocentric distance R is constant over the interval of a few days during which we make our measurements. Of course this is not true, but it is a pretty good approximation – the geocentric distance to the asteroid does constantly change but slowly, so that over an interval of a couple of nights we can pretend that it is constant.

The next key assumptions relate to the asteroid's orbital motion. They are:

- The geocentric rates in right ascension and declination will be assumed to be constant (linear motion) over an interval of a couple of days.
- We will estimate these orbital rates by using topocentric measurements at the moment of the asteroid culmination (when diurnal parallax is null).
- We will ignore any differences in the asteroid topocentric and geocentric declinations at the moment of transit (in practice, the real difference is usually insignificant).

From these three assumptions, at least in first approximation the asteroid orbital motion (geocentric coordinates) can be determined at any time from topocentric measurements as:

$$\alpha_{geo}(t) \approx \alpha_0 + \upsilon t = RA_0 + \upsilon t \qquad (14)$$

$$\delta_{geo}(t) \approx \delta_0 + \mu t \approx Dec_0 + \mu t \qquad (15)$$

where the asteroid right ascension constant rate ν is defined as

$$\upsilon = \frac{RA_{0_2} - RA_{0_1}}{T_{0_2} - T_{0_1}} \quad (16)$$

and the asteroid declination constant rate μ is defined as

$$\mu = \frac{Dec_{0_2} - Dec_{0_1}}{T_{0_2} - T_{0_1}} \qquad (17)$$

where RA_{01} and RA_{02} are the asteroid topocentric right ascensions respectively at the moment of the first (T_{01}) and second (T_{02}) transit times, while Dec_{01} and Dec_{02} are the asteroid topocentric declinations respectively also at the moment of the first (T_{01}) and second (T_{02}) transit times.

Thus substituting in Equation 12 it becomes

$$\tan(\Delta RA) = \frac{X\cos(Dec_0 + \mu t)\sin(RA_0 + \upsilon t) - \sin(\omega t)}{X\cos(Dec_0 + \mu t)\cos(RA_0 + \upsilon t) - \cos(\omega t)} \qquad (18)$$

This is the fundamental equation of our model. Once the key parameters T_0 and RA_0 become known, the left term is directly measurable by the observer at any given time, while in the right term – except for the geocentric asteroid distance R – all of the remaining parameters are either known a priori (R_E, λ, ω) or are also directly measurable by the observer (Dec_0, ν, μ). In consequence, the asteroid distance can be determined by applying an iterative process to a set of observations as follows:

1. From observed topocentric coordinates the asteroid linear orbital motion is determined, and hence the asteroid geocentric coordinates can be estimated at any given time.
2. Knowing the asteroid orbital motion and assuming a certain (guessed) asteroid distance, the model predicts for any given time what the topocentric right ascension has to be.
3. The distance value that best minimizes all RA residuals (observed minus model predicted topocentric right ascensions) for the given set of observations becomes the asteroid distance.

4. Determination of the Key Parameters T_0, RA_0 and Dec_0

The asteroid's exact local transit time T_0 has to be known as precisely as possible. An error of just one second does make difference. This fact imposes a hard restriction on the timing accuracy and therefore the easy shortcut of getting T_0 from published asteroid ephemerides is not an option.

Fortunately, T_0 can be easily determined by the observer at the required accuracy. The way to do this is by taking a set of images while the asteroid is around transit time (preferably from a couple of minutes before up to a couple of minutes after transit time). For each image, the corresponding time has to be accurately known and target astrometry has to be precisely measured. Then, the difference between measured RA of the asteroid to Local Sidereal Time can be determined for each observation time of the set of images. Finally, by using the Intercept function on a spreadsheet the time of transit T_0 and corresponding RA_0 and Dec_0 can be precisely obtained.

Having determined from observations made on two proximate nights (the adjacent, the better) corresponding parameters T_0, RA_0 and Dec_0, then the asteroid's geocentric orbital motion in right ascension and declination can be conveniently represented, at least in first approximation, by linear rates ν and μ just derived from those six parameters.

5. The RA Geocentric Linear Assumption

The quality of the diurnal parallax angle determination is based on two main subjects: (a) the accuracy of RA topocentric values actually measured, and (b) the accuracy of RA geocentric values estimated for the required parallax computation.

As already discussed, our (self-contained) model uses a linear approximation for the unknown RA geocentric values, so that asteroid distances can be truly determined from just the observer's data. However, replacing a curve by a linear approximation always introduces some error.

In case the time frame we consider is just two consecutive nights and the target asteroid is near opposition, then the asteroid does have an almost linear motion against the background stars and our linear assumption is totally pertinent – even though it's also the time of greatest motion in right ascension. In a more general situation, or for a longer time frame (let´s say 3-4 days) the real asteroid trajectory in-

creasingly departs from a linear motion. Could the error derived from the linear simplification still be manageable in a more general context?

The problem to solve is to somehow minimize the error derived by the replacement of the unknown general RA geocentric motion curve by a linear approximation. The linear approximation is the uniform rate ν that the observer is able to derive from the only two points (T_{01}, RA_{01} and T_{02}, RA_{02}) of the real RA geocentric curve that he can actually measure on just two proximate nights.

Of course, if the observer could be able to observe along several nights he would collect several pairs of (T_0 , RA_0) data points, which in turn makes it possible to derive a more accurate variable (time-dependent) rate for the real RA geocentric motion – instead of a simple uniform rate, finding out a first, second or even third order analytical expression for ν(t) . The same goes in case the observer could know such data from accurate target ephemerides. We are dealing here with the most likely – and easiest – case where the observer dedicates just two (partial) nights to find out the distance to a particular asteroid exclusively by means of his own data.

The graph in Figure 4 poses the question. If the real RA geocentric curve were to be replaced by just a linear approximation, then along one single observing session any "new" RA geocentric values would be either underestimated or overestimated by the simplification (the larger the time apart from the transit time T_0, the worse). Also for the same observing session, all RA geocentric values prior to the transit time would be replaced in the opposite way as those RA geocentric values after the transit time (if the former became underestimated, the latter resulted overestimated, or vice versa).

It becomes clear that working with a linear RA geocentric rate and using data from just one observing session obtained entirely from one side of the Meridian (either only prior or only after transit time) will achieve the largest error. To minimize diurnal parallax errors derived from the use of data from only one observing session it is necessary to observe the target for a long time both sides of the Meridian.

However, we found out an elegant simplification. Instead of observing the asteroid for a full night from dusk to dawn, and also at transit time on the following day, as shown in Figure 5 basically the same exactitude can be achieved if the target is observed on the two nights just from the same side of the Meridian.

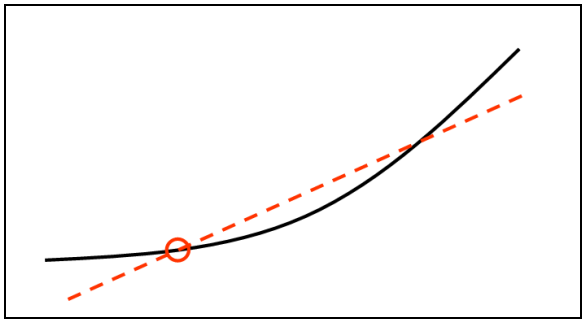

Figure 4: The problem with the linear assumption. Replacing a real curve by a linear approximation introduces errors in a particular direction previous to the point where the segment actually coincides with the curve, and in the opposite direction after such coinciding point.

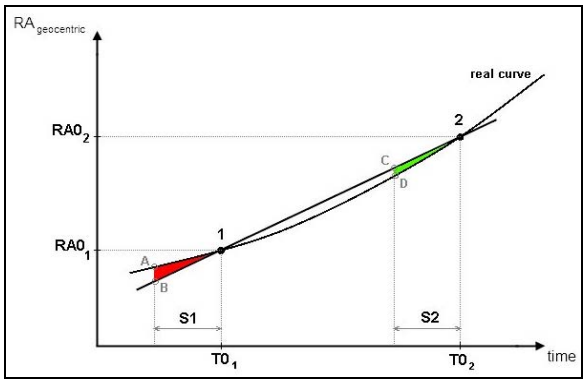

Figure 5: Replacing the real RA geocentric curve by a linear approximation makes the "new" RA values at any time previous to transit time (T_0) to be wrong in one direction for the first session (underestimated as shown in the red area for Session #1) but wrong in the opposite direction for the following session (overestimated as shown in the green area for Session #2).

Therefore, despite the fact that the RA geocentric values for each session necessarily are going to be inexact (the larger the curvature, the greater the error), if the observer only collects data either before or after the transit time, but not simultaneously from both sides, then the error introduced by the linear RA geocentric simplification tends to cancel out.

Using data from just one side of the Meridian not only means the observer does not need to work all night long (not a minor issue for amateurs committed to full-day jobs) but also implies that the asteroid no longer has to be near opposition (it could transit at any time during the night). Of course far from opposition the asteroid will be fainter and may follow a much more complicated trajectory – thus most likely decreasing the properness of the linear rate approximation – but on the other hand (a) the asteroid could be observed for a longer time frame than the 4-5 hours from dusk to midnight, or from midnight to dawn, and consequently (b) the asteroid could also be

observed for longer periods while comparatively at higher altitudes on the sky.

6. The Model At Test

We have applied the model to five different asteroids, trying to cover a wide distance spectrum. One close and fast moving NEO asteroid was observed having a large diurnal parallax angle (greater than 120 arcsec), three asteroids were observed at intermediate distances, and one last asteroid was observed at such a challenging far distance that its diurnal parallax angle (less than 3 arcsec) was as small as the local atmospheric blurring effect (seeing).

All observations were performed from Observatorio Los Algarrobos, Salto, Uruguay (MPC I38) at latitude -31º 23' 33", using a 0.3-m telescope and CCD camera yielding an image scale of 1.9 arcsec/pixel. MPO Canopus was the software used for astrometry.

All observed asteroids happened to be relatively close to their opposition date. We observed our five targets at least on one pair of consecutive nights, accumulating 10 pairs of such sessions. Except for one, all individual observing sessions lasted more than 4 hours. For each target we obtained a series of images taken about 15 minutes apart, except at each opening session and close to target culminations – when several images were taken continuously in order to improve derived astrometry accuracy. On some occasions we not only imaged the target for many hours prior to its culmination, but also for many hours after having past the Meridian as well.

6.1 Asteroid 8106 Carpino

This main belt asteroid was our first target, observed on two consecutive nights (2011, April 6 and 7) while exactly at opposition (April 7th) when it appeared with a visual magnitude of 15.5 and a phase angle of 9.9 degrees. Almost all observations of both sessions were made prior to transit time. Figure 6 shows the measured parallax angles assuming a linear RA geocentric motion derived from data collected on those nights.

Technical data for each session and corresponding values are summarized in Table I.

The distance derived from each session data was excellent (better than 4%). As expected, one value was underestimated while the other was overestimated. The found distance derived from the two sessions was remarkably good (2.5%). This proves the full validity of the RA "constant rate" assumption for the asteroid motion at opposition and the predicted trend for errors to cancel out if working with observations from just one side of the Meridian.

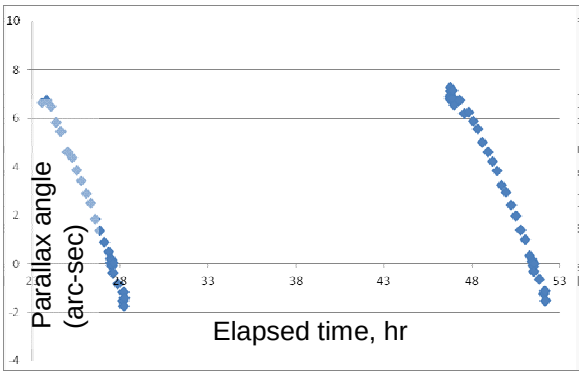

Figure 6: Observed 8106 Carpino's diurnal parallax by assuming asteroid RA linear motion, from data obtained on two consecutive nights (2011 April 6 and 7), which happened to coincide with its opposition date.

8106 Carpino	*Session #1*	*Session #2*	***Sess. 1&2***
Observation date (UT)	2011-04-06	2011-04-07	
Lapse to/from opposit (day)	-1	0	
True Distance (AU)	0.974	0.972	**0.973**
Phase Angle (deg)	9.94	9.91	
Visual magnitude (mag)	15.53	15.53	
Observed lapse before T0 (h)	4.0	4.8	
Observed lapse after T0 (h)	0.7	0.7	
Used RA rate	***Constant: v = -0.010151 arcsec/sec***		
Found Parallax (arcsec)	7.88	7.41	**7.52**
Found Distance (AU)	0.951	1.011	**0.997**
Relative error (%)	-2.4	+4.0	**+2.5**

Table I: 8106 Carpino Results

6.2 Asteroid 819 Barnardiana

This main belt asteroid was observed on three pairs of consecutive nights (2011, May 29-30, June 1-2, and June 11-12), that is, increasingly apart from opposition (May 19th) when it appeared with a visual magnitude of 13.6 and a phase angle of 5.2 degrees. We tried on this target several different and mixed combinations of prior/after transit observations. Figures 7-9 present the measured parallax angles for each pair of consecutive nights assuming a linear RA geocentric motion derived from data collected on corresponding nights.

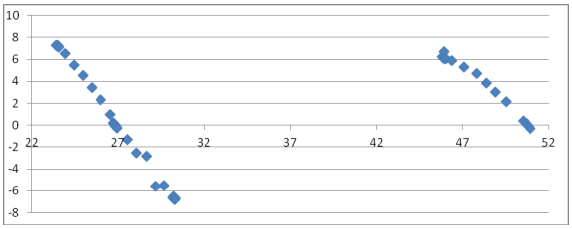

Figure 7: Observed 819 Barnardiana's diurnal parallax by assuming asteroid RA linear motion, from data obtained on two consecutive nights (2011 May 29 and 30), about ten days past opposition.

819 Barnardiana	*Session #1*	*Session #2*	***Sess. 1&2***	*Session #3*	*Session #4*	***Sess. 3&4***	*Session #5*	*Session #6*	***Sess. 5&6***
Observation date (UT)	2011-05-29	2011-05-30		2011-06-01	2011-06-02		2011-06-11	2011-06-12	
Lapse to/from opposit (day)	+10	+11		+13	+14		+23	+24	
True Distance (AU)	0.939	0.940	**0.940**	0.943	0.944	**0.944**	0.967	0.970	**0.969**
Phase Angle (deg)	7.83	8.24		9.21	9.70		14.32	14.81	
Visual magnitude (mag)	13.75	13.77		13.82	13.84		14.06	14.08	
Observed lapse before T0 (h)	3.5	5.0		4.5	4.7		2.8	3.4	
Observed lapse after T0 (h)	3.5	0.1		1.5	0.7		4.0	5.0	
Used RA rate	***Constant: v = -0.0104803 arcsec/sec***			***Constant: v = -0.0097799 arcsec/sec***			***Constant: v = -0.0064872 arcsec/sec***		
Found Parallax (arcsec)	8.93	6.51	**7.81**	10.20	6.13	**8.22**	10.13	4.55	**6.60**
Found Distance (AU)	0.840	1.152	**0.961**	0.731	1.223	**0.912**	0.740	1.644	**1.135**
Relative error (%)	-10.5	+22.6	**+2.2**	-22.5	+29.6	**-3.4**	-23.5	+69.5	**+17.1**
Used RA rate	***Variable (3rd order) rate***								
Found Parallax (arcsec)	7.14	7.33	**7.23**	8.05	7.80	**7.93**	7.95	8.16	**8.08**
Found Distance (AU)	1.050	1.023	**1.037**	0.931	0.961	**0.946**	0.943	0.919	**0.928**
Relative error (%)	+11.8	+8.8	**+10.3**	-1.3	+1.8	**+0.2**	-2.5	-5.3	**-4.2**

Table II: Conditions and results for 810 Barnardiana

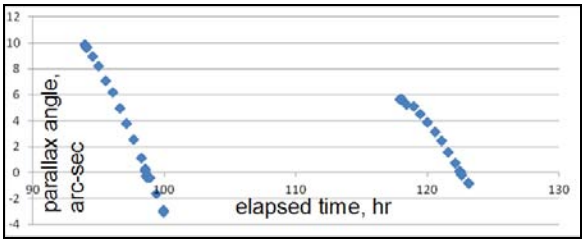

Figure 8: Observed 819 Barnardiana's diurnal parallax by assuming asteroid RA linear motion, from data obtained on two consecutive nights (2011 June 1 and 2), some 14 days past opposition.

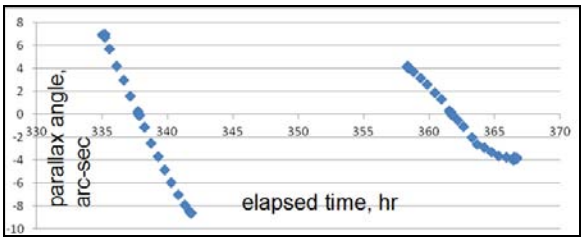

Figure 9: Observed 819 Barnardiana's diurnal parallax by assuming asteroid RA linear motion, from data obtained on two consecutive nights (2011 June 11 and 12), some 24 days past opposition.

It seems quite evident that for each pair of obtained parallactic curves, the shape of the first compared to the second become increasingly deformed. This is due to the linear RA geocentric assumption, which gradually loses validity as the asteroid moves away from opposition. This is made manifest by observing how the linear rate changed from an almost-similar value for the first pair of nights compared to the last value – respectively, 0.0105, 0.0098 and 0.0065 arcsec/sec, that is, the linear rate for the last pair was only 60% of the first one, thus approaching the highly curved part of its orbital trajectory when the asteroid switches between prograde and retrograde motion. For those sessions that covered a large time on both sides of the Meridian, some deformation of the diurnal parallax curves becomes evident – notoriously in Figure 9. Despite the diurnal parallax effect being a totally symmetric phenomenon, the "uniform RA rate" assumption introduces errors that make the angle to appear increased at one side of the Meridian and diminished at the other, so that the shape distortion becomes worse as the asteroid trajectory increases its curvature, i.e., as the asteroid gets farther from opposition.

Having observed this target on six sessions distributed half-month apart, from our own data we were able to find out a much better representation of the actual RA geocentric motion of the asteroid. Figures 10-12 show the same collected data as before, but this time a variable (third order) rate has been used for the RA geocentric trajectory. One glance at Figures 9 and 12, which are based on the same data, is enough for understanding the matter.

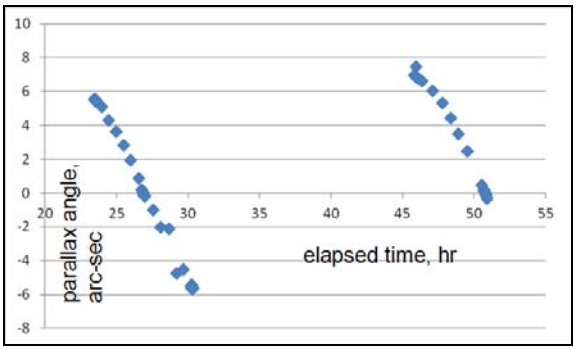

Figure 10: Observed 819 Barnardiana's diurnal parallax by assuming asteroid RA variable (3rd order) motion, from data obtained on two consecutive nights (2011 May 29 and 30), about ten days past opposition.

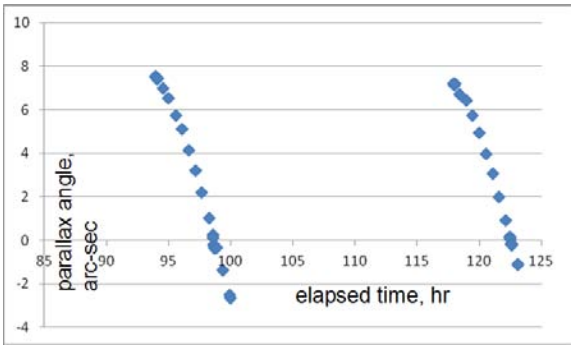

Figure 11: Observed 819 Barnardiana's diurnal parallax by assuming asteroid RA variable (3rd order) motion, from data obtained on two consecutive nights (2011 June 1 and 2), some 14 days past opposition.

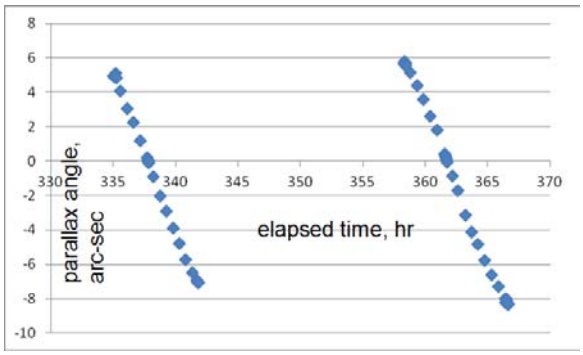

Figure 12: Observed 819 Barnardiana's diurnal parallax by assuming asteroid RA variable (3rd order) motion, from data obtained on two consecutive nights (2011 June 11 and 12), some 24 days past opposition.

Technical data for each session and corresponding values are summarized in Table II.

Using the linear approximation we obtained mediocre results if considering only data from each night; however, outcomes from considering the joint data of each pair of nights were again excellent (better than 3.5%) for the first and second pairs (those closer to opposition), although poor (17%) for the last one (24 days past opposition). On the other hand, using a quadratic approximation for the whole considered period we obtained very good results (better than 5%) either for the individual sessions as well as for the pairs, except for the first one (10%). Logically, the variable rate expression rectifies the problem where the trajectory wasn't uniform, and worsens where the motion was actually practically linear. One last fact worth mentioning is that the two larger errors from combined nights also occurred for those pairs (first and third) when one of the sessions covered a large span on one side of the Meridian not covered by the other.

6.3 The Far Away Asteroid 414 Liriope

This challenging outer main belt asteroid was observed on three pairs of consecutive nights (2011, August 30-31, September 1-2, and September 5-6), that is, increasingly apart from opposition (August 25th) when it appeared with a visual magnitude of 14.5 and a phase angle of 2.5 degrees. We also tried on this target several different and mixed combinations of prior/after transit observations. Unfortunately, the third session was aborted half hour prior transit time due to cloud covering. Figures 13, 14 and 15 present the measured parallax angles for each pair of consecutive nights assuming a linear RA geocentric motion derived from data collected on corresponding nights.

The computation of the exact transit time for the third session (2011-09-01) couldn't be done as usual (from data collected around asteroid culmination from that session) so that it had to be derived from previous and following observations. The quality of the obtained data is clearly inferior to those from previous targets, something totally expected given the small parallactic angles now in play.

Technical data for each session and corresponding values are summarized in Table III.

414 Liriope	*Session #1*	*Session #2*	***Sess. 1&2***	*Session #3*	*Session #4*	***Sess. 3&4***	*Session #5*	*Session #6*	***Sess. 5&6***
Observation date (UT)	2011-08-30	2011-08-31		2011-09-01	2011-09-02		2011-09-06	2011-09-07	
Lapse to/from opposit (day)	+5	+6		+7	+8		+12	+13	
True Distance (AU)	2.544	2.545	**2.545**	2.546	2.548	**2.547**	2.557	2.558	**2.558**
Phase Angle (deg)	2.92	3.10		3.29	3.51		4.48	4.49	
Visual magnitude (mag)	14.56	14.58		14.59	14.60		14.67	14.67	
Observed lapse before T0 (h)	4.9	5.1		4.6	5.2		4.9	4.7	
Observed lapse after T0 (h)	0.1	0.1		N/A	0.8		0.7	1.0	
Used RA rate	***Constant: v = -0.0070355 arcsec/sec***			***Constant: v = -0.0069983 arcsec/sec***			***Constant: v = -0.0067985 arcsec/sec***		
Found Parallax (arcsec)	2.82	2.79	**2.80**	3.30	2.91	**3.05**	2.88	2.56	**2.85**
Found Distance (AU)	2.660	2.692	**2.674**	2.273	2.579	**2.460**	2.604	2.874	**2.627**
Relative error (%)	+4.6	+5.8	**+5.1**	-10.7	+1.2	**-3.5**	+1.8	+12.4	**+2.7**
Used RA rate	***Variable (3rd order) rate***								
Found Parallax (arcsec)	2.65	2.97	**2.81**	2.93	2.89	**2.91**	2.75	2.98	**2.81**
Found Distance (AU)	2.830	2.525	**2.668**	2.559	2.595	**2.577**	2.727	2.516	**2.678**
Relative error (%)	+11.2	-0.8	**+4.8**	+0.5	+1.8	**+1.1**	+6.6	-1.6	**+4.7**

Table III: Circumstances and results for 414 Liriope

Despite the small parallax angle – approaching the frontier where measurement reliability becomes degraded – outcomes from the linear assumption were still very good (around 5%) for the first pair of sessions and even better (better than 3.5%) for the other two pairs.

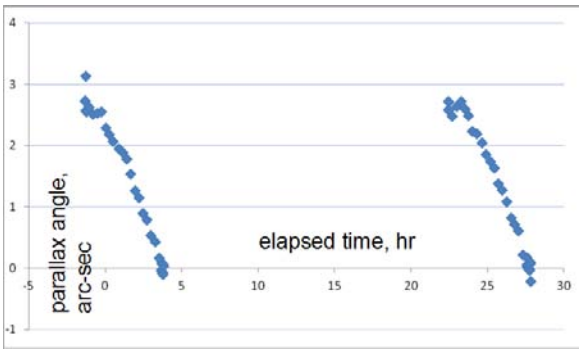

Figure 13: Observed 414 Liriope's diurnal parallax by assuming asteroid RA linear motion, from data obtained on two consecutive nights (2011 August 30 and 31), some 5 days past opposition.

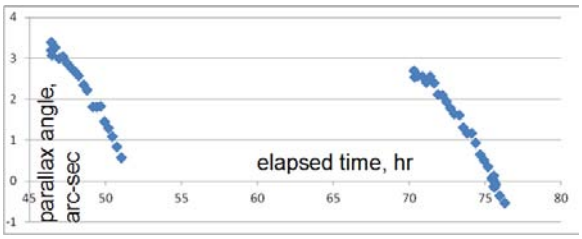

Figure 14: Observed 414 Liriope's diurnal parallax by assuming asteroid RA linear motion, from data obtained on two consecutive nights (2011 September 1 and 2), some 8 days past opposition.

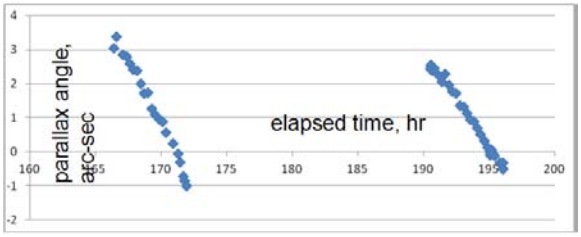

Figure 15: Observed 414 Liriope's diurnal parallax by assuming asteroid RA linear motion, from data obtained on two consecutive nights (2011 September 6 and 7), some 13 days past opposition.

6.4 Asteroid 1660 Wood

This main belt asteroid was observed on four consecutive nights (2012, January 23-24-25-26) prior to opposition (January 29th) when it appeared with a visual magnitude of 13.4 and a phase angle of 24.6 degrees. Sessions were relatively short (all under 5.5 hours, while the 3.7 hour session from 2012-01-24 was the shortest one for this work). Figures 16 and 17 present the measured parallax angles for each pair of consecutive nights assuming a linear RA geocentric motion derived from data collected on corresponding nights.

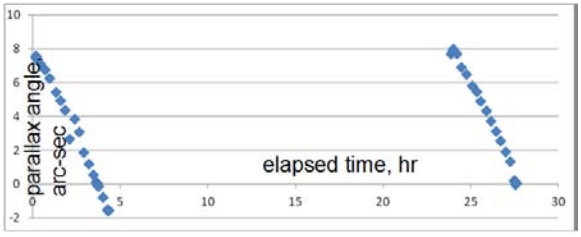

Figure 16: Observed 1660 Wood's diurnal parallax by assuming asteroid RA linear motion, from data obtained on two consecutive nights (2012 January 23 and 24), some 5 days prior to opposition.

1660 Wood	*Session #1*	*Session #2*	***Sess. 1&2***	*Session #3*	*Session #4*	***Sess. 3&4***
Observation date (UT)	2012-01-23	2012-01-24		2012-01-25	2012-01-26	
Lapse to/from opposit (day)	-6	-5		-4	-3	
True Distance (AU)	0.831	0.830	**0.831**	0.829	0.828	**0.829**
Phase Angle (deg)	24.74	24.71		24.64	24.60	
Visual magnitude (mag)	13.76	13.76		13.75	13.75	
Observed lapse before T0 (h)	3.5	3.7		3.8	3.8	
Observed lapse after T0 (h)	0.7	0.0		1.7	1.5	
Used RA rate	***Constant: v = -0.0074036 arcsec/sec***			***Constant: v = -0.0072342 arcsec/sec***		
Found Parallax (arcsec)	9.45	9.70	**9.58**	9.59	8.32	**8.92**
Found Distance (AU)	0.793	0.773	**0.783**	0.782	0.901	**0.840**
Relative error (%)	-4.6	-6.9	**-5.8**	-5.7	+8.8	**+1.3**

Table IV: Circumstances and Results for 1660 Wood

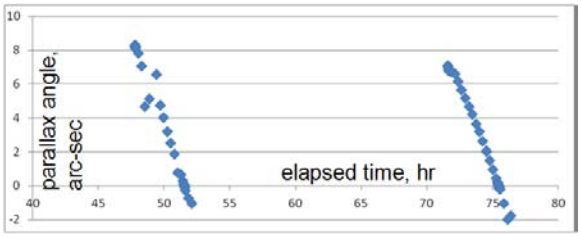

Figure 17: Observed 1660 Wood's diurnal parallax by assuming asteroid RA linear motion, from data obtained on two consecutive nights (2012 January 25 and 26), some 3 days prior to opposition.

Despite working with short-span data, outcomes for combined sessions were very good (5.8% and 1.3%). The fact that we got (twice) data from three nights in a row allowed us to compare results for the same central night – but derived from two different uniform rates – one applying the linear motion from the adjacent first and central nights, and another from the also adjacent central and last nights of the trio. For the 2012-01-25 session we obtained a distance of 0.885 AU (+6.8%) and 0.781 AU (-5.8%) if we applied the different linear rates measured for each pair of days of the trio (respectively, -0.007404 and -0.007315 arcsec/sec). That is, a mere 1.2% in difference in the assumed uniform RA geocentric rate caused a 12.6% difference in the derived asteroid distance, for data just 4 days away from opposition.

6.5 The Close Asteroid (162421) 2000 ET70

This NEO (Athen) asteroid was observed on two consecutive nights (2012, February 22-23) coinciding with its opposition (February 22nd) when it appeared with a visual magnitude of 13.2 and a phase angle of 40.7 degrees. The rapid sky displacement of this neighbor while visiting us at opposition (-0.2644 arcsec/sec) posed some practical problems (varying star background context from where astrometry was obtained) not previously dealt with. Figure 18 presents the measured parallax angles for the pair of consecutive nights using the "linear RA geocentric motion" assumption, derived from data collected on these nights.

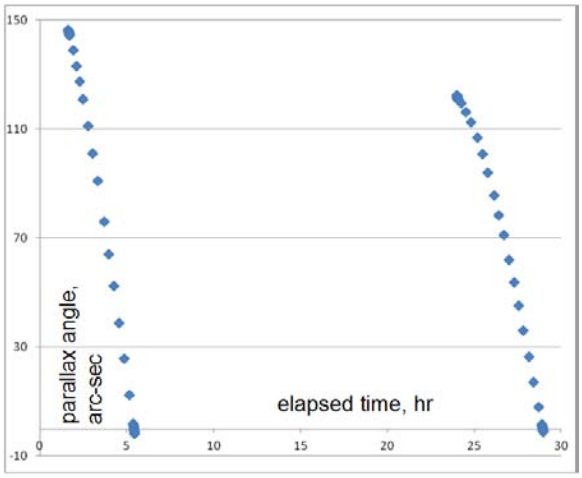

Figure 18: Observed (162421) 2000 ET70's diurnal parallax by assuming asteroid RA linear motion, from data obtained on two consecutive nights (2012 February 22 and 23), which happened to coincide with its opposition date.

Besides the rapid sky motion, the closeness of the asteroid also implied a large diurnal parallax effect. Hence, absolute measurement errors comparatively became less important, which neatly explains the cleanness of the obtained parallactic curves. Considering that except at the beginning and at transit of each session each data point was obtained at approximately the same intervals, the curves not only show how the parallactic angle actually changed with time, but also its variable rate of change.

The asteroid distance obtained from the combined session was quite good (6%), derived from the two sessions with large individual errors (-10.4 and

(162421) 2000 ET70	*Session #1*	*Session #2*	***Sess. 1&2***
Observation date (UT)	2012-02-22	2012-02-23	
Lapse to/from opposit (day)	0	1	
True Distance (AU)	0.048	0.050	**0.049**
Phase Angle (deg)	40.80	41.90	
Visual magnitude (mag)	13.27	13.41	
Observed lapse before T0 (h)	3.8	5.0	
Observed lapse after T0 (h)	0.0	0.0	
Used RA rate	***Constant: v = -0.2644330 arcsec/sec***		
Found Parallax (arcsec)	172.6	125.9	**145.0**
Found Distance (AU)	0.043	0.060	**0.052**
Relative error (%)	-10.4	+20.0	**+6.1**

Table V: Circumstances and Results for (162421) 2000 ET70

+20.0%). One important matter for this close flying-by target is that at opposition, its geocentric distance was changing by about 4% per 24-h, which obviously violates the crucial "constant distance" assumption in our model.

6.6 Discussion of Results

Target	RA rate Model	*Sess. 1&2*	*Sess. 3&4*	*Sess. 5&6*
8106 Carpino	uniform	+2.5	-	-
819 Barnardiana	uniform	+2.2	-3.4	+17.1
819 Barnardiana	variable (3rd order)	+10.3	+0.2	-4.2
414 Liriope	uniform	+5.1	-3.5	+2.7
414 Liriope	variable (3rd order)	+4.8	+1.1	+4.7
1660 Wood	uniform	-5.8	+1.3	-
(162421) 2000 ET70	uniform	+6.1	-	-

Table VI: Distance percent errors for each one of the combined consecutive sessions

Table VI summarizes final asteroid distances derived from observational data. Distances from combined consecutive nights' data were very good, even for the challenging 2.5 AU far away asteroid. Some measurements for 819 Barnardiana gave the largest errors, due to the fact that observations at first and third pairs of sessions were collected on both sides of the Meridian. The NEA asteroid gave the worst case, but the obtained 6.1% error distance was also surprisingly good, given its rapidly-changing distance.

The adopted asteroid's geocentric rate in RA is critical for an accurate determination of its distance derived from the diurnal parallax effect. Results are very sensitive to the RA geocentric rate that was actually used. Depending on asteroid distance and orbital position, a tiny percent change in the assumed RA rate can change the calculated asteroid distance by far more than ten times such percent.

The linear RA geocentric assumption has been proven useful and effective. Results derived from the more accurate "variable rate" model became marginally superior in the case when 819 Barnardiana was far away from opposition. On this scenario, the a single observer can still accurately determine the distance to an asteroid all by his own by observing the target at transit along a handful of nights, so that he can obtain a good model of the changing RA geocentric rate.

7. A Much Simpler Stratagem

We also applied our data to Equation 1. Assuming that the distance to a far away target remains constant, and that there is almost no variation in declination for the short considered daily interval, the diurnal parallax angle varies in a sinusoidal way as

$$\varphi(t) \approx A\sin(\omega_T t) \tag{19}$$

where the amplitude A is the maximum diurnal parallax angle (ω_T) is the angular rate of the sine curve and the time variable (t) is selected exactly the same way as before (its beginning coincides with the moment of the asteroid's culmination).

The maximum diurnal parallax angle A corresponds to the parallactic value 6 hours either before or after transit, and becomes the key value for finding out the distance. In theory, it could be possible to directly measure it but it requires the asteroid to be far way from opposition (which poses the problem of the variable RA geocentric rate); in practice, the difficulty of accurately measuring such a small angle (usually less than 10 arcsec) turns the direct attempt almost impossible. However, it is possible to determine it indirectly.

From equations 1 and 19 we have

$$[RA_{topo}(t) - \alpha_{geo}(t)]\cos\delta(t) \approx A\sin(\omega_T t) \tag{20}$$

From our data, at the time of each observation we know the asteroid topocentric coordinates, as well as corresponding RA geocentric value. The angular rate of the sine curve can be readily derived from our observations at two consecutive transit times, becoming

$$\omega_T = \frac{2\pi}{T_{0_2} - T_{0_1}} \tag{21}$$

Therefore, by finding the A value that best minimizes all residuals in Equation 20 for a given set of observations (the same process applied in our previous model to Equation 18, this time trying to determine the sinusoidal curve that best fits the left-side data term in Equation 20) the maximum parallactic angle is determined and yields the distance to the object once the baseline ($R_E\cos\lambda$) is applied to Equation 2.

Asteroid distances obtained by using the simplification of Equation 20 applied to exactly the same observational data already presented were virtually identical to those obtained through our more rigorous model. This wasn't a surprise as both models are basically solving the same geometry, but anyway it was a general validity for Equation 19.

Finally, we tried an even more intrepid bet. Instead of dealing with a large set of observations for

finding the amplitude of the parallactic sine curve, we tried using only four data points: those from the beginning and around transit time for each of two consecutive nights. This ultimate simplification to an already simple method proved to be totally pertinent, as results were only marginally poorer than those obtained from our (much more complex) model. Just four data points strategically selected (those at zero-level parallactic angle and those as large as possible from the same side of the Meridian) are sufficient for accurately finding out the amplitude of the diurnal parallax effect.

In order to improve the quality of the results, in practice the data-points far away from culmination should be obtained as a set of several consecutive images – the same procedure as for accurately determining transit times.

Distance percent errors from combined consecutive sessions, by means of our model, the sine curve simplification, and "the 4-Point shortcut" (as we have named it) are shown in Table VII.

The innovative 4-Point shortcut for determining an asteroid distance is self-contained, extremely simple (only requiring two observations on consecutive nights), and yields very good accuracy (around 5% or better) on condition the asteroid is fairly close to opposition. If that is not the case, some more data is required (observations from a few more nights, but only done at transit times).

	The formal model		
Target	***Sess. 1&2***	***Sess. 3&4***	***Sess. 5&6***
8106 Carpino	+2.5	-	-
819 Barnardiana	+2.2	-3.4	+17.1
414 Liriope	+5.1	-3.5	+2.7
1660 Wood	-5.8	+1.3	-
(162421) 2000 ET70	+6.1	-	-

	The sine curve simplification		
Target	***Sess. 1&2***	***Sess. 3&4***	***Sess. 5&6***
8106 Carpino	+2.5	-	-
819 Barnardiana	+2.1	-3.4	+17.2
414 Liriope	+5.2	-3.5	+2.9
1660 Wood	-5.8	+1.4	-
(162421) 2000 ET70	+6.1	-	-

	The 4-POINT ultimate simplification		
Target	***Sess. 1&2***	***Sess. 3&4***	***Sess. 5&6***
8106 Carpino	+1.8	-	-
819 Barnardiana	+4.0	-3.8	+3.7
414 Liriope	+6.4	-	+2.2
1660 Wood	-5.8	0.0	-
(162421) 2000 ET70	+4.1	-	-

Table VII: Comparison of Results from Three Methods

8. Range of Distances

By means of a modest 0.30-m telescope we have successfully tested the 4-Point shortcut method for determining asteroid distances up to 2.5 AU – which implied dealing with a parallactic angle about 3 arcsec without any problem. Working with similar sized, good optics telescopes, in principle we don't see any limitation preventing the detection of a ten times lesser parallactic angle if due care, proper image scale, and favorably seeing conditions are all in play.

From equations 2 and 3, the corresponding distance in AU for a parallactic angle of 0.3 arcsec equals 29.2 times the cosine of the observer's latitude. Therefore, we think the distance determination of bright enough Solar System objects up to 20-25 AU by means of a backyard telescope applying the 4-POINT shortcut is a feasible task – although a certainly challenging one. We are planning some experiments to see if we can measure the distance to Pluto with this method.

9. Stellar Parallax

The distance to nearby stars can be accurately determined by measuring their parallax angle while the Earth orbits around the Sun. The geometry of this situation is exactly the same as drawn in Figure 1, where now the circumference represents the orbit of the Earth. As the Earth orbits around the Sun, any observer on its surface sees the star's parallactic angle φ constantly varying, from a maximum value occurring whenever the Earth is at right angle to the plane perpendicular to the Ecliptic which also contains both the Sun and the star (some 3 months prior or after star due opposition) to a null value whenever the Earth happens to also be placed on such plane (star opposition).

If the beginning of the time parameter is strategically selected to coincide with the moment of the star opposition, then our reasoning for the diurnal parallax effect is completely valid for the star parallax case – and therefore all the equations of our model can be accordingly translated. The former exact time of the asteroid culmination now becomes the exact time of the star opposition; the former unknown geocentric motion of the asteroid now becomes the unknown proper motion of the star.

Therefore, the 4-Point shortcut for the distance determination of a nearby star should work all the same, except this time to collect the four data points will take 15 months instead of just 30 hours.

Considering that the parallax angle of nearby stars is within reach of backyard observers (Sirius has a parallax of about 0.38 arcsec), once again the determination of their distance by means of the 4-Point shortcut should be a challenging but feasible task – although not especially suitable for the impatient observers.

10. Conclusions

For asteroids (or other Solar System objects) our method for determining their diurnal parallax and hence their distance is both simple and sensitive, only requiring two measurements on two proximate nights (the more adjacent, the better) from just one single observing point. On each night one of the measurements must be done around the time of culmination and the other as far from culmination as possible, in order to maximize sensitivity; but on both sets of measurements should be taken from the same side of the Meridian.

Achieving a distance accuracy of 5% for an asteroid close to opposition, derived from nothing other than just backyard observations from a single station during a short time interval – about 30 hours – is remarkable and totally feasible. The cherry on the top is that this goal – a kind of amateur fantasy not so long ago – only demands two sets of asteroid images, each covering not more than ten minutes, taken on two consecutive nights.

11. References

Buchheim, R. K. (2011) "A Modern Incarnation of Tycho's Diurnal Parallax Method." in *Proceedings for 31st Annual Symposium on Telescope Science* (Warner et al., eds.) pp. 109-114. Society for Astronomical Sciences, Rancho Cucamonga, CA.

Forbes, E. G. (1976). "Early Astronomical Researches of John Flamsteed." *Journal for the History of Astronomy* **7**, 124-138.

Lindsay, L., Gill, D. (1877) "Note on the results of heliometer observations of the planet Juno, to determine its diurnal parallax." *Monthly Notices of the Royal Astronomical Society* **37**, 04/1877, 308.

Ratcliff, S. J., Balonek, T. J., Marschall, L.A., DuPuy, D. L., Pennypacker, C. R., Verma, R., Alexov, A., Bonney, V. (1993). "The measurement of astronomical parallaxes with CCD imaging cameras on small telescopes." *American Journal of Physics* **61**, 208-216.

Smallwood, L. M., Katz, D. M., Richmond, M. W. (2004). "Near Earth Objects: A Brief Review and A Student Project." *American Journal of Physics* **72**, 264-279.

Vanderbei, R. J., Belikov, R. (2007). "Measuring the Astronomical Unit." *Sky and Telescope* January 2007, 91-94.